*Acta Cryst.* (1961). **14**, 1250

# The Crystal Structure of Potassium Hydrogen Maleate

By S. F. Darlow

*Crystallographic Laboratory, Cavendish Laboratory, Cambridge, England*
*and *Physics Department, College of Science and Technology, Manchester 1, England*

and W. Cochran

*Crystallographic Laboratory, Cavendish Laboratory, Cambridge, England*

(*Received* 23 *March* 1961)

Potassium hydrogen maleate [$K^+(^-OOC.CH=CH.COOH)$] crystallizes in the orthorhombic space group *Pbcm*, with 4 molecules per unit cell and cell dimensions

$$a = 4{\cdot}578 \pm 0{\cdot}002,\ b = 7{\cdot}791 \pm 0{\cdot}004,\ c = 15{\cdot}953 \pm 0{\cdot}005\ \text{Å}.$$

800 independent reflections were recorded photographically, each intensity being measured visually four or eight times. Refinement proceeded by three-dimensional difference methods to a residual of 4·9%, with anisotropic temperature parameters applied to the five independent potassium, oxygen and carbon atoms. The structure consists of alternate layers of $K^+$ cations and planar hydrogen maleate anions, each cation being eight-fold coordinated to the oxygens of the anions. The anions are chelate, and the internal hydrogen bond has a length of 2·437 ± 0·004 Å. The hydrogen electron-density sections are consistent with a symmetrical hydrogen bond.

## Introduction

Potassium hydrogen maleate (abbreviated to KH*M*) is an acid salt of maleic acid. The $HM^-$ ion is shown in Fig. 1. Maleic acid has the form of a chelate ring with a very short internal hydrogen bond of length 2·46 ± 0·02 Å (Shahat, 1952). From the asymmetry of the maleic acid molecule it was concluded that this bond is definitely not symmetrical. Cardwell, Dunitz & Orgel (1953) deduced from an infra-red study that the internal hydrogen bond is stronger in the $HM^-$ ion than in maleic acid, and probably symmetrical, since the infra-red spectrum of KH*M* cannot be explained as a superposition of carboxyl group and carboxylate ion vibration modes.

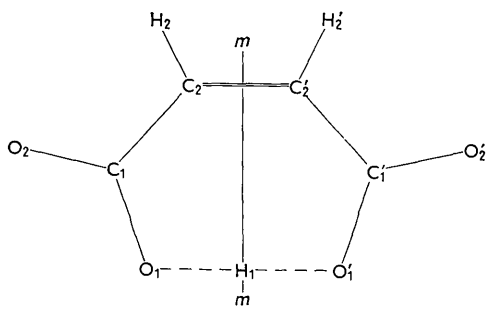


Fig. 1. The hydrogen maleate ion, showing the space group mirror plane and the labelling used.

The crystal structure of KH*M* was investigated in an attempt to decide on the nature of this hydrogen bond and to determine accurately the dimensions of the anion. Cardwell *et al.* gave the space group as orthorhombic, $Pbc2_1$ or *Pbcm*, with

$$a = 4{\cdot}54,\ b = 7{\cdot}78,\ c = 15{\cdot}95\ \text{Å},$$

a molecular weight of 154, a density of 1·82 g.cm.$^{-3}$ and 4 molecules per unit cell.

* Present address.

## The (100) and (010) projections

The 0*kl* and *h*0*l* reflections were recorded out to $\sin\theta/\lambda = 0{\cdot}95$, firstly with a Weissenberg camera using Cu $K\alpha$ and Mo $K\alpha$ radiation and later with a Geiger-counter diffractometer (Cochran, 1950) with Mo $K\alpha$ radiation. The film data were obtained by visual comparison with standard scales; the residual between the film and counter structure factors was 3·7%. In the 0*kl* zone 114 intensities out of 152 were measured, and 84 out of 101 for *h*0*l*. The projections were solved from the Patterson functions, using the space group *Pbcm*, which is centrosymmetrical with eight general equivalent positions. The $K^+$ ions are on diads parallel to *a* and the $HM^-$ ions are parallel to the *c* axis, each anion being positioned symmetrically across the space-group mirror plane at $z = \frac{1}{4}$ or $\frac{3}{4}$ (see Fig. 3). The presence of a mirror plane does not prove that the hydrogen bond is symmetrical (as shown in Fig. 1), since it might be only statistically symmetrical, cf. potassium hydrogen dibenzoate (Skinner, Stewart & Speakman, 1954).

Both projections were refined by difference methods, with anisotropic temperature factors applied to every atom except the hydrogens, and the 0*kl* and *h*0*l*

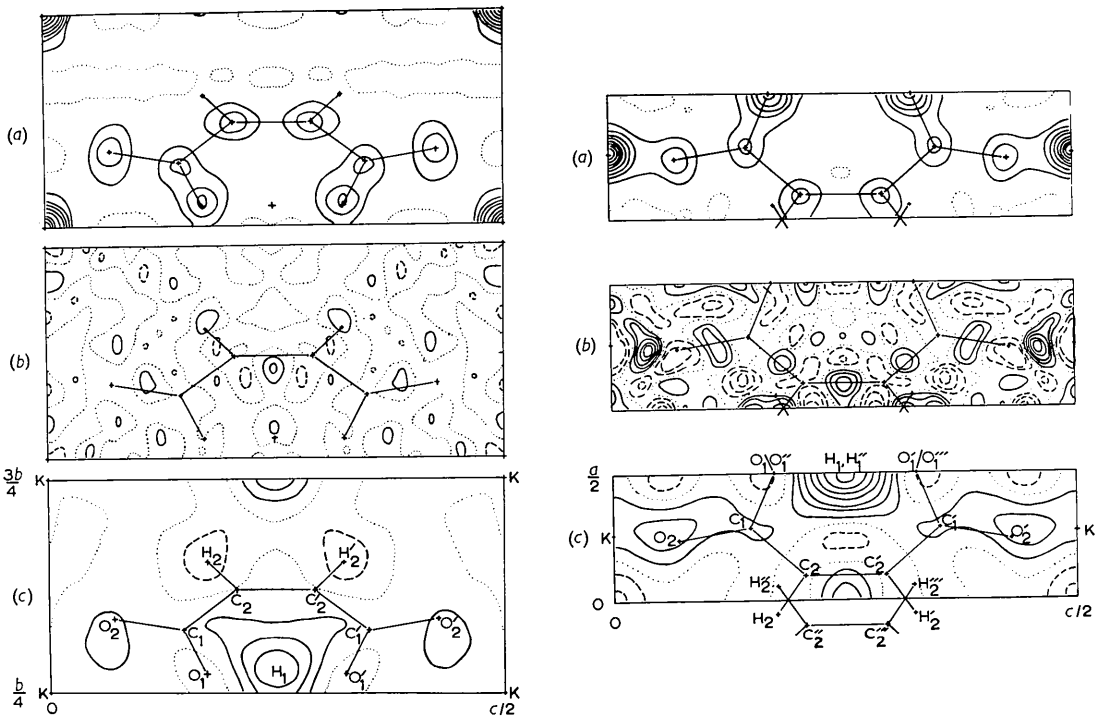


Fig. 2. The final 0*kl* (left-hand column) and *h*0*l* (right-hand column) (*a*) observed electron density, (*b*) outer difference, and (*c*) inner difference maps. Maps (*c*) include $H_1$ and the $HM^-$ electron. The contours are on an arbitrary scale, with the difference contours at (1/20)th the interval of the electron density contours. Full line, positive; dotted line, zero; broken line, negative.

residuals (including the 'unobserved' reflections) decreased to 4·2 and 8·7%, $H_1$ being omitted from the calculated structure factors. All atoms were completely resolved in the (100) projection, and $O_1$ and the hydrogens were the only overlapped atoms for *h*0*l*. In the later stages of refinement only the outer terms with $\sin\theta/\lambda \geq 0{\cdot}355$ were used so that the hydrogens and any extinction effects would not distort the structural parameters of the other atoms (Jellinek, 1958*a*, *b*). Absorption corrections were applied, being in the range 0·704 to 0·771 for the crystal used for the 0*kl* measurements and 0·767 to 0·856 for the other. The *h*0*l* residual was considered unsatisfactory, but some of the *h*0*l* spots were slightly split and it was assumed that the crystal used was not perfect. As a full three-dimensional analysis was planned these data were not re-measured with a different crystal. Fig. 2 shows the final (*a*) observed electron density (*b*) outer difference and (*c*) inner difference maps. In maps (*c*) $H_1$ and the $(HM)^-$ electron have not been subtracted. Although spurious detail can be seen in the *h*0*l* 'outer difference' map, the final *z* coordinates determined from each projection had a maximum difference of only 0·006 Å.

## Three-dimensional refinement

The original *a* axis crystal and a needle-shaped crystal with length parallel to *c* were used to record photographically three-dimensional data in layers with $0 \leq h \leq 4$, $0 \leq l \leq 6$ and $l=8$ using a Weissenberg camera in the equi-inclination setting with Mo $K\alpha$ radiation. Approximately 800 independent reflections out of a possible 1,200 with $\sin\theta/\lambda \leq 0{\cdot}85$ were visually measured. Roughly half of these were recorded about both axes and their intensities measured eight times. The others were measured four times. Phillips' (1956) spot shape correction was applied to the 'extended' intensities and the 'contracted' intensities were then scaled to these and a mean taken. The empirical scaling curves used for the 'contracted' intensities fitted the expression given by Phillips for large $\sin\theta$ but at low $\sin\theta$ it did not apply, as expected. The residual between the intensities derived from the extended spots and those from the contracted spots was 6·5%, and this was taken as a measure of their random errors.

For the first cycle of refinement the final projection coordinates were used. Thermal ellipsoids were estimated for each atom from the two projections but were subject to large errors. Hydrogen atoms were included with isotropic temperature factors, but their parameters were not refined. The atomic form factors given by Berghuis *et al.* (1955) were used for $K^+$, C and O, and that of Viervoll & Øgrim (1949) for hydrogen.

The layers of observed structure factors were on different scales and, since the intensities had been

estimated by eye and the spot shape varied with $\sin\theta$ due to beam divergence, crystal shape and $\alpha_1\alpha_2$ resolution as well as the higher-layer effect, they were each scaled separately to the calculated structure factors using scaling curves which varied smoothly with $\sin\theta$. The scaling curves were refined with the structural parameters, thus introducing approximately an extra 25 parameters. The final curves had reasonable shapes with only one maximum or minimum each, and it was considered that fewer systematic errors were introduced this way. This method may not be used if data have been collected about one axis only, as errors in temperature factors can then largely be compensated by the scaling curves. After scaling in layers the $a$ and $c$ axis data were averaged together.

Refinement proceeded as follows. Sections through the three-dimensional electron density were computed and showed that the $x$ coordinate of $O_1$ (the only coordinate affected by overlap in either projection) was in error by 0·09 Å. An ellipsoid was deduced for each atom by measuring the contour diameters in each section through the atomic centres. The ellipsoids deduced in this way were found to fit non-central sections, at least qualitatively, although sections through carbon atoms showed anomalies which could be ascribed to bonding. In order to relate the semi-axial lengths ($S_X$, $S_Y$, $S_Z$) of an electron-density ellipsoid to the semiaxial lengths ($B_X$, $B_Y$, $B_Z$) of the corresponding temperature factor ellipsoid it was assumed that Booth's (1946) approximation for the electron density could be applied to an atom at rest. Convolution with the probability distribution function of the atom then leads to

$$\left.\begin{aligned} B_X &= (S_X/S_Z)^2 B_Z + 4\pi^2[(S_X/S_Z)^2 - 1]/p \\ B_Y &= (S_Y/S_Z)^2 B_Z + 4\pi^2[(S_Y/S_Z)^2 - 1]/p \end{aligned}\right\} \quad (1)$$

(see Appendix I), where $p$ is the constant used in Booth's approximation. Thus if $p$ and either one of the $B$ values or their average is known, the $B_X$,$B_Y$ and $B_Z$ values may be calculated from $S_X : S_Y : S_Z$. The value of $p$ calculated from the oxygen $f$-curve was 46 Å$^{-2}$ (Appendix II), but equation (1) is not very sensitive to $p$, and so values close to this were assumed for all the atoms.

Equation (1) now gave the new temperature parameters. In subsequent cycles of refinement, sections through the three-dimensional difference density were computed, using outer terms only ($\sin\theta/\lambda \geq 0{\cdot}355$). From the theory in Appendix I the equation

$$\Delta B_r = [2\pi^2/\varrho(0)][(1/p) + (B_r/4\pi^2)]^2[\delta^2 D(0)/\delta r^2] \quad (2)$$

was deduced for the change in the temperature parameter $B_r$, where $r$ is an ellipsoid axis, $\varrho(0)$ is the central electron density of the observed Fourier map and $[\delta^2 D(0)/\delta r^2]$ is the central curvature in the $r$ direction on the difference map. Equation (2) was assumed to be approximately true for any direction. It is again not very sensitive to the value of $p$ used. In practice it was found in the course of the refinement that values of $\Delta B$ estimated in this way were relatively correct, but were too small by a factor of about two. This is probably explained by the method of scaling, which partially masks the effect of wrong values of $B$ by changes to the scaling curves for different layers. These curves should of course refine with the $B$ parameters.

The fourth cycle of refinement gave difference sections through the atomic positions which showed very few features, the largest value of $|D|$ being 0·4 e.Å$^{-3}$, compared with 1·1 e.Å$^{-3}$ for the second cycle and peak heights on the first cycle Fourier sections of 54·8 e.Å$^{-3}$ for $K^+$ and 10–14 e.Å$^{-3}$ for the other atoms. The refinement was terminated at this stage; it had reduced the residual for the outer terms from 9·7 to 5·8%. The final coordinates and temperature factors are shown in Tables 1 and 2. The hydrogens contributed appreciably only to the inner terms, and are discussed later.

Table 1. *Final fractional coordinates, with the projection values in brackets*

| | $x$ | | $y$ | | $z$ | |
|---|---|---|---|---|---|---|
| $K^+$ | 0·2615 | (0·2617) | 0·7500 | (0·7500) | 0·0000 | (0·0000) |
| $O_1$ | 0·4851 | (0·5000) | 0·2958 | (0·2959) | 0·1737 | (0·1738) |
| $O_2$ | 0·2360 | (0·2370) | 0·4200 | (0·4201) | 0·0719 | (0·0723) |
| $C_1$ | 0·2845 | (0·2825) | 0·3969 | (0·3969) | 0·1471 | (0·1480) |
| $C_2$ | 0·0904 | (0·0915) | 0·4885 | (0·4885) | 0·2078 | (0·2077) |

Extinction corrections were applied using the method of Vand (1955) with $[(c/2)F_c^2(000)] = 0{\cdot}160$ and 0·329 for the $a$ and $c$ axis data respectively. Only the inner reflections were affected, and after re-scaling the inner residual decreased from 5·6 to 3·4%, the residual for all the reflections decreasing to a final value of 4·9%. As a check on the method of scaling, the residuals between the scaled $a$ and $c$ sets of data for the first and fourth cycles were computed. They were 7·8 and 6·3%, indicating that the scaling curves had improved with the other parameters.

Table 2. *Final temperature parameters*

| | $r$ | $B_r$ | $r\frown a$ | $r\frown b$ | $r\frown c$ |
|---|---|---|---|---|---|
| $K^+$ | $X$ | 2·85 Å$^2$ | 0° | 90° | 90 |
| | $Y$ | 2·80 | 90 | 10 | 80 |
| | $Z$ | 2·45 | 90 | 100 | 10 |
| $O_1$ | $X$ | 2·93 | 40·5 | 121·7 | 67·6 |
| | $Y$ | 5·07 | 53·1 | 37·6 | 96·1 |
| | $Z$ | 2·36 | 104·3 | 72·0 | 23·3 |
| $O_2$ | $X$ | 4·65 | 10·2 | 99·0 | 94·6 |
| | $Y$ | 3·77 | 80·4 | 12·7 | 81·9 |
| | $Z$ | 2·04 | 86·8 | 98·8 | 9·4 |
| $C_1$ | $X$ | 3·09 | 20·5 | 105·4 | 103·2 |
| | $Y$ | 2·35 | 74·7 | 15·5 | 92·4 |
| | $Z$ | 2·03 | 76·7 | 91·2 | 13·4 |
| $C_2$ | $X$ | 3·08 | 35·4 | 54·7 | 87·3 |
| | $Y$ | 2·43 | 125·4 | 35·5 | 87·6 |
| | $Z$ | 2·67 | 90·8 | 93·5 | 3·6 |

### Estimation of errors

Since the data were measured out to the same reciprocal radius in all directions, Cruickshank's (1960) method for calculating the standard deviations of the structural parameters was used, and gave:

$$\text{oxygens } \sigma(r)=0{\cdot}0017 \text{ Å}, \quad \sigma(B)=0{\cdot}04-0{\cdot}07 \text{ Å}^2,$$
$$\text{carbons } \sigma(r)=0{\cdot}0019 \text{ Å}, \quad \sigma(B)=0{\cdot}05-0{\cdot}07 \text{ Å}^2.$$

As the $K^+$ cations are on diad axes, they were given the values

$$\sigma(x)=0{\cdot}002 \text{ Å}, \quad \sigma(B)=0{\cdot}05 \text{ Å}^2.$$

The method of scaling may have introduced some systematic errors in the temperature factors, and the $\sigma(B)$ values quoted above are doubtless too optimistic (Lonsdale & Milledge, 1961). No simple estimate of errors for the ellipsoid angles can be given, but any angle changes which do not alter the value of $B$ in any direction by more than 0·14 Å$^2$ may be considered within the limits of possible error.

In view of the above accuracy it was decided to re-measure the cell parameters. Cu $K\alpha$ zero-layer Weissenberg photographs were taken about each axis using a fresh crystal, which was replaced for part of each exposure by a rock-salt powder specimen of similar absorption factor to calibrate the films. From the sin $\theta$ values of ten high angle reflections the cell parameters were calculated to be

$$a=4{\cdot}578\pm0{\cdot}002, b=7{\cdot}791\pm0{\cdot}004, c=15{\cdot}953\pm0{\cdot}005 \text{ Å}.$$

Only the value of $a$ was very significantly different (by $19\sigma$) from the value given by Cardwell *et al.* (1953).

In order to calculate bond-length standard deviations the formula for $\sigma(l)$ given by Ahmed & Cruickshank (1953) was extended to include the effect of errors in cell parameters, and became

$$\sigma^2(l)=\sum_i \{\cos^2\alpha_i[\sigma^2(x_{i1})+\sigma^2(x_{i2})] + (l/a_i)^2\cos^4\alpha_i\sigma^2(a_i)\}, \quad (3)$$

where $l$ is the length of the bond between atoms 1 and 2, $\cos\alpha_i$, $x_i$ and $a_i$ are the direction cosines, atomic coordinates and cell dimensions respectively in the $i$th direction, and $i=1, 2$ and 3. The $\sigma^2(a_i)$ terms in equation (3) proved to be negligible for all bond lengths, and their effect on the bond angle standard deviations (Darlow, 1960) was omitted.

### Details of the structure

The structure (Fig. 3) is composed of alternate layers of $K^+$ and $HM^-$ ions, the anions being oriented so that there are sheets of oxygens on either side of the potassium layers. The potassiums are in an approximately hexagonal array, with K–K distances 4·466, 4·572 and 4·578 ± 0·003 Å and K–$\hat{K}$–K angles of 58·4, 60·7 and 60·9 ± 0·2°. Fig. 4 shows the environment of each atom, together with the thermal ellipsoid axes and $B$ values. The potassium stereogram includes the eight nearest oxygens, six of type $O_2$ and two of type $O_1$, labelled with superscripts 1 to 8. The following tables give the K–O distances and O–$\hat{K}$–O angles:

Table 3. K–O *distances*

| Oxygens | (Å) | Oxygens | (Å) |
|---|---|---|---|
| $O_2$ 1, 4 | 2·817 ± 0·003 | $O_2$ 5, 6 | 2·873 ± 0·003 |
| $O_2$ 2, 3 | 2·891 ± 0·003 | $O_1$ 7, 8 | 3·025 ± 0·003 |

Table 4. $O^n$–K–$O^m$ *angles*

| Oxygens ($n$, $m$) | Angle (°) | Type |
|---|---|---|
| 2, 3 | 74·6 ± 0·4 | *A* |
| 5, 6 | 75·1 ± 0·4 | *A* |
| 1, 2; 3, 4 | 77·1 ± 0·2 | *A* |
| 1, 6; 4, 5 | 73·1 ± 0·2 | *A* |
| 2, 7; 3, 8 | 43·7 ± 0·2 | *A* |
| 4, 7; 1, 8 | 75·6 ± 0·2 | *A* |
| 6, 7; 5, 8 | 83·4 ± 0·2 | *A* |
| 1, 3; 2, 4 | 106·8 ± 0·3 | *B* |
| 1, 5; 4, 6 | 103·1 ± 0·3 | *B* |
| 3, 5; 2, 6 | 105·2 ± 0·2 | *B* |
| 1, 7; 4, 8 | 106·3 ± 0·2 | *B* |
| 3, 7; 2, 8 | 106·4 ± 0·2 | *B* |
| 5, 7; 6, 8 | 136·4 ± 0·2 | *B* |
| 2, 5; 3, 6 | 180 ± 0·4 | *C* |
| 1, 4 | 175·3 ± 0·5 | *C* |
| 7, 8 | 134·9 ± 0·5 | *C* |

For regular eight-fold coordination the angles of types *A*, *B* and *C* would be 70·5, 109·5 and 180° respectively. The main deviations are caused by the $O_1$ atoms being rigidly bound to the $O_2$ atoms in the $HM^-$ ions, and the slight anisotropy of the $K^+$ ion

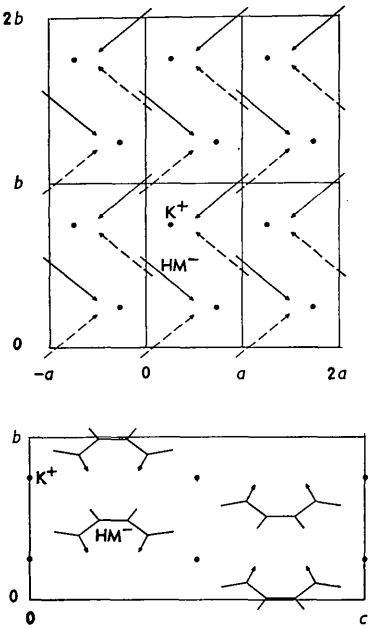


Fig. 3. Projections of the structure perpendicular to the $c$ and $a$ axes. The dots represent potassiums. In the top figure the $HM^-$ ions are seen end-on, with those in full lines above the plane of the potassiums and those in broken lines below The arrow heads indicate $O_1$ and $O_1'$.

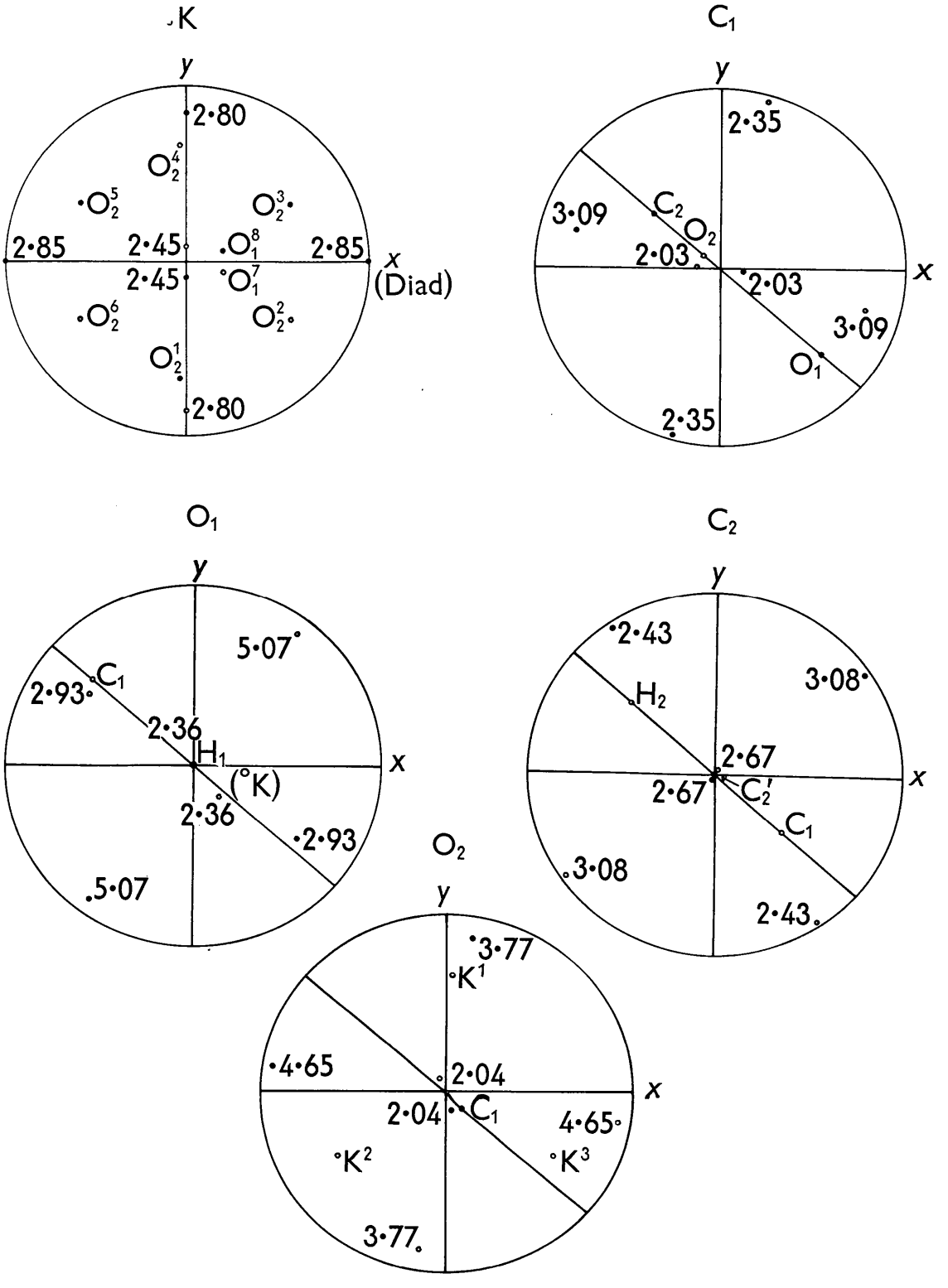


Fig. 4. Stereographic projections down the *c* axis of the bonding and thermal vibration ellipsoid axes for the $K^+$ cation and the atoms in the $HM^-$ ion labelled in Fig. 3. The oblique line through each pole represents the plane of the $HM^-$ ion. The values of *B* are given in Å$^2$.

is consistent with these deviations. It can be seen from Fig. 3 that the planes of the anions almost go through the potassiums, and this has the effect of minimizing the K–$O_1$ distances and maximizing the (2, 7) angle of 43·7°. It may be concluded that the packing of the $O_2$ atoms round the potassiums gives the positions of the H$M^-$ ions while their orientations are governed by the fitting of the $O_1$ atoms close to the $K^+$ ions and the anions into one another.

The H$M^-$ ion is planar, with a least-squares plane

$$0{\cdot}2000x+0{\cdot}2402y=1\,, \qquad (4)$$

where $x$ and $y$ are coordinates in Å. This plane is marked on the stereograms in Fig. 4. The deviations from this plane are small but significant, namely

| | |
|---|---|
| $O_1$ −0·007 Å | $C_1$ +0·010 Å |
| $O_2$ +0·007 Å | $C_2$ −0·010 Å . |

These suggest that the ion is slightly bent about an axis parallel to $c$ passing near $C_1$ and $O_2$. The difference between 0·007 and 0·010 Å is not meaningful.

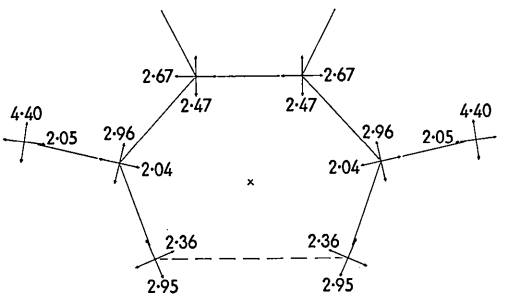


Fig. 5. The $B$ values (in Å² units) of the sections of the thermal ellipsoids in the plane of the anion.

$O_2$ has approximately tetrahedral coordination with $3K^+$ ions and $C_1$. All the angles are within 12° of 109·5°. The atomic anisotropies are in general consistent with the bonding, but suggest a libration of the anion in its own plane. The temperature factors in this plane are shown in Fig. 5, and suggest an oscillation about the point marked × with a mean displacement angle of 3·2°. The anisotropy of $C_2$ is rather small, but the bond-length corrections (Cruickshank, 1956) are only of the order of the standard deviations, namely 0·004 Å for $O_1O_1'$, 0·003 Å for $C_1C_2$ and 0·002 Å for $C_1O_1$, $C_1O_2$ and $C_2C_2'$. The bond lengths and angles of the H$M^-$ ion are shown in Fig. 1 of the following paper (Darlow, 1961) where they are discussed in detail.

## Discussion of the hydrogens

The three-dimensional difference sections for $H_1$ and $H_2$ (Fig. 6) were computed using the terms with $\sin\theta/\lambda<0{\cdot}55$ ($H_1$ and $H_2$ being omitted from the calculated structure factors). The peak densities are 0·70 and 0·98 e.Å$^{-3}$ compared with the calculated value of 0·89 e.Å$^{-3}$ for $B=3$ Å². For comparison, the average background over all the unit cell is 0·13 e.Å$^{-3}$. The $H_2$ maps are centred on the point of maximum electron density with coordinates (0·9379, 0·5571, 0·1812) giving a C–H bond length of 0·976 Å. A standard deviation of 0·02 Å was arbitrarily assumed for this length. $H_2$ is $-(0{\cdot}05\pm0{\cdot}02)$ Å from the mean H$M^-$ plane, consistent with the small bend in the anion.

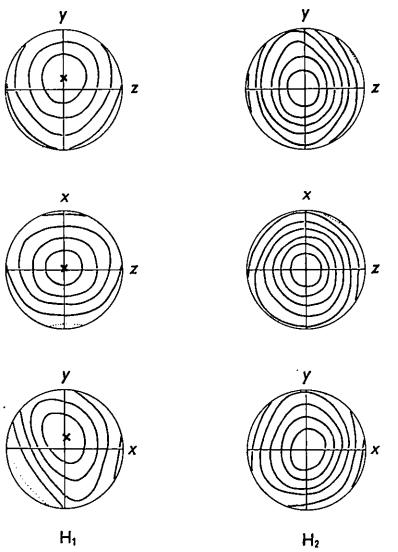


Fig. 6. Final difference sections for $H_1$ and $H_2$. The circles have diameters of 1·25 Å, and the maps have either the zero or first contours as the lowest ones shown, with a contour interval of 0·14 e.Å$^{-3}$.

$H_1$ has a lower peak density than $H_2$, as is commonly found for hydrogens in hydrogen bonds. The $H_1$ sections in Fig. 6 are centred on the midpoint of the $O_1O_1'$ line, but the peak density position (marked with a cross) is 0·11 Å from this midpoint in a direction at 45° to the H$M^-$ plane with the component in the plane towards the centre of the ring. This is unexpected, and is probably not significant since the density at the midpoint of $O_1O_1'$ is only 0·02 e.Å$^{-3}$ less than the maximum value. Whilst the anisotropy of $H_1$ may not be significant either, it is in the opposite direction to that expected, since the oxygens $O_1$ and $O_1'$ have a large motion perpendicular to the molecular plane whereas $H_1$ has apparently the smallest motion in this direction. This is discussed in the following paper.

No definite conclusion can be drawn as to the nature of the hydrogen bond, but the $H_1$ electron distribution is consistent with a centred hydrogen model.

This structure was first presented (in projection only) at the Symposium on Hydrogen Bonding held at Ljubljana, Yugoslavia, in July 1957, the Symposium proceedings being published in 1959 (Darlow, 1959). The $0kl$ projection has been independently solved by Peterson & Levy (1958) using neutron diffraction. They obtained a value of 2·44 Å for the $O_1H_1O_1'$ bond and also found a larger thermal motion

of $O_1$ perpendicular to the bond compared with $H_1$. A full three-dimensional neutron analysis would provide an interesting comparison with our results.

## APPENDIX I

Consider an atom with centre at the origin of coordinates. Let $(X, Y, Z)$ be the coordinates of a point in real space relative to the principal axes of the vibration ellipsoid of the atom, and $(u, v, w)$ be the coordinates of a point in reciprocal space relative to the principal axes of the thermal ellipsoid of the atom. Let the Fourier transform of the electron distribution in the atom be

$$f(u, v, w) = f_0(u, v, w) \exp\left[-(B_X u^2 + B_Y v^2 + B_Z w^2)/4\right], \quad (I{\cdot}1)$$

where $f_0(u, v, w)$ is the spherically symmetrical transform of the spherically symmetrical electron density $\varrho_0(X, Y, Z)$ for the atom at rest, and

$$[(B_X u^2 + B_Y v^2 + B_Z w^2)/4]$$

represents the thermal ellipsoid. Then the electron distribution $\varrho(X, Y, Z)$ is given by the convolute of $\varrho_0(X, Y, Z)$ with $P(X, Y, Z)$ the probability distribution function for the atom, where

$$P(X, Y, Z) = (64\pi^3/B_X B_Y B_Z)^{\frac{1}{2}} \times \exp\left[-4\pi^2(X^2/B_X + Y^2/B_Y + Z^2/B_Z)\right] \quad (I{\cdot}2)$$

is the Fourier transform of

$$\exp\left[-(B_X u^2 + B_Y v^2 + B_Z w^2)/4\right],$$

(Cochran, 1954). Booth's (1946) approximation for the atomic shape (here taken for an atom at rest) then gives

$$\varrho(X, Y, Z) = \iiint_{-\infty}^{\infty} \{Z(p/\pi)^{3/2} \exp\left[-p\{(X+X')^2 + (Y+Y')^2 + (Z+Z')^2\}\right] (64\pi^3/B_X B_Y B_Z)^{1/2} \times \exp\left[-4\pi^2(X'^2/B_X + Y'^2/B_Y + Z'^2/B_Z)\right]\} dX'\, dY'\, dZ' . \quad (I{\cdot}3)$$

Re-arranging leads to

$$\varrho(X, Y, Z) = Z(64p^3/B_X B_Y B_Z)^{1/2} \times \int_{-\infty}^{\infty} \exp\left[-\{p(X+X')^2 + (4\pi^2/B_X)X'^2\}\right] dX' \times \int_{-\infty}^{\infty} \exp\left[-\{p(Y+Y')^2 + (4\pi^2/B_Y)Y'^2\}\right] dY' \times \int_{-\infty}^{\infty} \exp\left[-\{p(Z+Z')^2 + (4\pi^2/B_Z)Z'^2\}\right] dZ', \quad (I{\cdot}4)$$

giving

$$\varrho(X, Y, Z) = Z(p/\pi)^{3/2}(C_X C_Y C_Z)^{1/2} \times \exp\left[-p(C_X X^2 + C_Y Y^2 + C_Z Z^2)\right], \quad (I{\cdot}5)$$

where

$$C_X = (1 + pB_X/4\pi^2)^{-1} \quad \text{etc.} \quad (I{\cdot}6)$$

Thus if $\varrho(X, Y, Z)$ has the same value for the axial points $(S_X, 0, 0)$, $(0, S_Y, 0)$ and $(0, 0, S_Z)$, then

$$C_X S_X^2 = C_Y S_Y^2 = C_Z S_Z^2,$$

which after re-arranging becomes

$$B_X = (S_X/S_Z)^2 B_Z + 4\pi^2[(S_X/S_Z)^2 - 1]/p$$

and

$$B_Y = (S_Y/S_Z)^2 B_Z + 4\pi^2[(S_Y/S_Z)^2 - 1]/p . \quad (I{\cdot}7)$$

This is equation (1).

Differentiating (I·5) and taking $X = Y = Z = 0$ gives

$$\partial^2\varrho(0)/\partial X^2 = -2pC_X\varrho(0) . \quad (I{\cdot}8)$$

For a difference section through the atomic centre, with

$$D = (\varrho_o - \varrho_c) \quad \text{and} \quad |D(0)/\varrho(0)| \ll 1 ,$$

(I·8) leads to

$$\partial^2 D(0)/\partial X^2 = -2p\varrho(0)(\partial C_X/\partial B_X)\Delta B_X ,$$

where $\Delta B_X = (B_{X,\,\text{obs.}} - B_{X,\,\text{calc.}})$, and using (I·6) gives

$$\Delta B_X = [2\pi^2/p^2 C_X^2 \varrho(0)][\partial^2 D(0)/\partial X^2] \quad \text{etc.} \quad (I{\cdot}9)$$

This is the basis of equation (2).

## APPENDIX II

For an isotropic atom, (I·5) becomes

$$\varrho_{r,\,B} = Z(p/\pi)^{3/2} C^{3/2} \exp\left[-pCr^2\right] = \varrho_{0,\,0} C^{3/2} \exp\left[-pCr^2\right] . \quad (II{\cdot}1)$$

Differentiating and taking $r = 0$ leads to

$$\partial^2\varrho_{0,\,B}/\partial r^2 = -2p\varrho_{0,\,0}C^{5/2} = (\partial^2\varrho_{0,\,0}/\partial r^2)C^{5/2} . \quad (II{\cdot}2)$$

Substituting (I·6) and re-arranging then gives

$$(-\partial^2\varrho_{0,\,B}/\partial r^2)^{-2/5} = (-\partial^2\varrho_{0,\,0}/\partial r^2)^{-2/5}[(p/4\pi^2)B + 1] . \quad (II{\cdot}3)$$

Thus a plot of $(-\partial^2\varrho_{0,\,B}/\partial r^2)^{-2/5}$ against $B$ should be a straight line with a ratio of slope to intercept of $(p/4\pi^2)$.

The curvature of the electron density function was obtained as follows:

$$\varrho_{r,\,B} = \int_0^{\infty} 4\pi s^2 f(s) \exp\left(-Bs^2/4\right) (\sin 2\pi rs/2\pi rs)\, ds , \quad (II{\cdot}4)$$

where $s = |2 \sin\theta/\lambda|$ ,

so that

$$\partial^2\varrho_{r,\,B}/\partial r^2 = (\partial^2/\partial r^2) \int_0^{\infty} 4\pi s^2 f(s) \times \exp\left(-Bs^2/4\right)[1 - (2\pi sr)^2/6 + 0(r^4)]\, ds$$

and hence

$$\partial^2\varrho_{0,\,B}/\partial r^2 = (-16\pi^3/3) \int_0^{\infty} [s^4 f(s) \exp\left(-Bs^2/4\right)]\, ds .$$

This may be approximated by

$$\partial^2\varrho_{0,\,B}/\partial r^2 = (-16\pi^3/3)\Delta s \sum_0^{s'} [s^4 f(s) \times \exp\left(-Bs^4/4\right)] . \quad (II{\cdot}5)$$

(II·5) was calculated for the oxygen $f$ curve, sampled at intervals of 0·1 out to $s'=2·6$. Values of $B$ were taken from 0 to 5 in steps of 1. The summations for $B=0$ and $B=1$ were not very convergent within the range used, but the values for $B=2$ to 5 gave $p=46$ Å$^{-2}$ from the graph of (II·3). This is the value used in equation (1).

Part of this work forms part of the Ph.D. thesis of one of us (S. F. D.). We are grateful to Prof. N. F. Mott, F. R. S., and Dr W. H. Taylor for the provision of research facilities, Dr M. V. Wilkes for permission to use EDSAC, Mr M. Wells for the use of many of his programmes and several members of the laboratory staff who have greatly assisted in the calculations. One of us (S. F. D.) acknowledges financial support from the Department of Scientific and Industrial Research. We should also like to thank Prof. J. Dunitz, who first drew our attention to this problem.

### References

Ahmed, F. R. & Cruickshank, D. W. J. (1953). *Acta Cryst.* **6**, 385.
Berghuis, J., Haanappel, IJ. M., Potters, M., Loopstra, B. O., MacGillavry, C. H. & Veenendaal, A. L. (1955). *Acta Cryst.* **8**, 478.
Booth, A. D. (1946). *Proc. Roy. Soc.* A, **188**, 77.
Cardwell, H. M. E., Dunitz, J. D. & Orgel, L. E. (1953). *J. Chem. Soc.*, p. 3740.
Cochran, W. (1950). *Acta Cryst.* **3**, 268.
Cochran, W. (1954). *Acta Cryst.* **7**, 503.
Cruickshank, D. W. J. (1956). *Acta Cryst.* **9**, 757.
Cruickshank, D. W. J. (1960). *Acta Cryst.* **13**, 774.
Darlow, S. F. (1959). *Hydrogen Bonding*, p. 37 (ed. Hadzi). London: Pergamon.
Darlow, S. F. (1960). *Acta Cryst.* **13**, 683.
Darlow, S. F. (1961). *Acta Cryst.* **14**, 1257.
Jellinek, F. (1958*a*). *Acta Cryst.* **11**, 627.
Jellinek, F. (1958*b*). *Acta Cryst.* **11**, 677.
Lonsdale, K. & Milledge, J. (1961). *Acta Cryst.* **14**, 59.
Peterson, S. W. & Levy, H. A. (1958). *J. Chem. Phys.* **29**, 948.
Phillips, D. C. (1956). *Acta Cryst.* **9**, 819.
Shahat, M. (1952). *Acta Cryst.* **5**, 763.
Skinner, J. M., Stewart, G. M. D. & Speakman, J. C. (1954). *J. Chem. Soc.*, p. 180.
Vand, V. (1955). *J. Appl. Phys.* **26**, 1191.
Viervoll, H. & Øgrim, O. (1949). *Acta Cryst.* **2**, 277.

*Acta Cryst.* (1961). **14**, 1257

# The Configuration of the Strained Hydrogen Maleate Ion

By S. F. Darlow

*Physics Department, College of Science and Technology, Manchester* 1, *England*

(*Received* 23 *March* 1961)

The strained configuration of the hydrogen maleate ion

$$HOOC.CH=CHCOO^-$$

in the potassium hydrogen maleate structure is investigated. It is shown that the strain energy is approximately 7·5 Kcal./mole, and the corrections to the bond lengths due to the strain are of the order of 0·01 Å. With these corrections, the carbon–carbon bond lengths are equal to the pure single- and double-bond lengths expected between carbons in the $sp^2$ state of hybridization.

In the preceding paper (Darlow & Cochran, 1961), the three-dimensional refinement of the structure of potassium hydrogen maleate has been described. In this paper the bond-lengths and angles of the hydrogen maleate ion ($HM^-$) in this structure are discussed. They are shown in Fig. 1 with the oscillation corrections added. The bond-length standard deviations do not include the oscillation correction uncertainties.

The ion is considerably strained in the planar cis configuration, and in Table 1 the experimentally determined angles are compared with the values expected for the corresponding unstrained angles. The symbols used for them in the following discussion are shown in brackets.

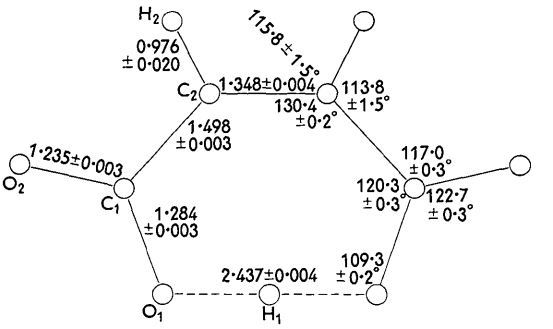


Fig. 1. The bond lengths and angles in the hydrogen maleate ion. The two halves of the ion are related by a mirror plane.